J Solid State Electrochem (2008) 12:1357–1365
DOI 10.1007/s10008-008-0577-4

ORIGINAL PAPER

Exploration of variables in the fabrication of pyrolysed photoresist

Callie Fairman · Samuel S. C. Yu · Guozhen Liu · Alison J. Downard · D. Brynn Hibbert · J. Justin Gooding

Received: 28 February 2008 / Accepted: 1 May 2008 / Published online: 3 June 2008

Abstract The increased use of pyrolysed photoresist films (PPF) as electrode material intensifies the need to know what fabrication variables are important in the pyrolysis process. The main factor effects of seven variables (three time/temperature heating levels plus the position in the furnace tube) in the fabrication of PPF were investigated by a Plackett and Burman, eight-run, experimental design. In the three-step pyrolysis programme, gas flow had a large effect on the surface cleanliness and roughness. It was also observed that the position in the furnace affected the resistivity of the PPF. Fabrication parameters that give rapid electron transfer to redox species in solution, that provide low surface oxide and that lead to low surface roughness were identified. The guidelines on what fabrication conditions to employ to give a variety of different electrode characteristics are presented.

Keywords Pyrolysed photoresist films · Carbon electrodes · Experimental design · Plackett–Burman design

Introduction

Glassy carbon (GC) is commonly used as an electrode material in electrochemical sensors as it has a wide potential window and is a very stable material under a wide range of conditions [1]. Carbon is a good electrode for most redox reactions and can be modified by reduction of various compounds (for an example, aryl diazonium salts [2, 3]) to form stable layers with suitably reactive groups for the attachment of sensing moieties. GC is made from the high-heat treatment of phenolic resins [4] and has domains of graphite in an amorphous phase consisting of entangled aromatic ribbons that are crossed linked with sp^3 bonding [5–7]. The drawback of GC is that the surface of the final material is rough on the molecular level. This roughness has implications for modern trends in sensing where molecular level control over the modification of an electrode surface is important [3]. Therefore, if the advantages of GC are to be exploited over as wide a range of potential applications as possible, then there is a need for smoother surfaces for molecular level control of the surface modification, for high-resolution patterning and for the atomic force microscopy (AFM) investigation into the layers formed by various surface modification techniques [8, 9]. An alternative to GC is thin carbon films. Previous studies by McCreery and co-workers [10] and the Kinoshita group [11] have shown that thin carbon films can be formed by the pyrolysis of photoresist films to give far smoother carbon surfaces than are achievable with conventional methods of fabricating GC (less than 0.5 nm compared with 4.5–44 nm for GC) [11, 12]. In common with surfaces of GC, films formed from this process are mainly amorphous with graphitic regions [13].

Pyrolysed photoresist films (PPF) are used as an alternative to GC for both electrochemical studies and to provide carbon surfaces for modification [14]. PPF is made from photoresist material used in the microfabrication industry. A thin film is laid down on a substrate and then pyrolysed in a tube furnace to give a conducting carbon film. The attractiveness of PPF is that it not only provides a much smoother surface but also has the good electrochemistry of GC and is compatible with bulk manufacture of a range of conducting carbon structures. PPF's

C. Fairman · G. Liu · D. B. Hibbert · J. J. Gooding (✉)
School of Chemistry, The University of New South Wales, Sydney 2052, Australia
e-mail: Justin.Gooding@unsw.edu.au

D. B. Hibbert
e-mail: B.Hibbert@unsw.edu.au

S. S. C. Yu · A. J. Downard
MacDiarmid Institute for Advanced Materials and Nanotechnology, Department of Chemistry, University of Canterbury, Christchurch 8140, New Zealand

have also been shown to have low oxygen content (O/C ratios of approximately 0.05 for films pyrolysed at temperatures greater than 700 °C) [11] and they are slow to be oxidised in ambient atmospheres [10]. The low O/C is important if these materials are to be used as microelectrodes and microbatteries, as the O/C ratio influences the electron transfer rate of some redox probes [10, 11].

We report here an initial study of the effects of changing the values of parameters which are important in the fabrication of PPF. The effect of the final pyrolysis temperature on PPF properties has been investigated by McCreery and co-workers [12], Lyons and co-workers [13, 15, 16] and Kinoshita and co-workers [11]. It has been shown that PPF prepared at pyrolysis temperatures of 1,000 to 1,100 °C has lower resistivity and faster electron transfer rates [17] than those prepared at lower temperatures. For $Fe(CN)_6^{3-/4-}$, ΔE_p at 800 °C is 277 mV, whilst at 1,100 °C, ΔE_p is 80 mV both at a scan rate of 200 mV s^{-1}, and for $Ru(NH_3)_6^{2+/3+}$, ΔE_p at 800 °C is 88 mV, whilst at 1,100 °C ΔE_p is 70 mV both at a scan rate of 200 mV s^{-1} [12]. The atmospheres in which the photoresist is pyrolysed have also been studied by McCreery and co-workers [12] and Lyons and co-workers [13, 15, 16], where it was observed that a low O/C ratio is produced in an atmosphere of 'forming gas' (95% N_2, 5% H_2). Madou and co-workers [17] and Lyons and co-workers [13] examined the initial thickness of the photoresist and found the resistivity was independent of film thickness when pyrolysed at 1,100 °C. Furthermore, a positive photoresist is preferred as less film shrinkage is observed when pyrolysed compared with negative photoresist [18, 19], and graphite-like areas begin to form at lower temperatures in positive photoresist films (600 °C) than in negative photoresist films (2,700 °C) [18, 19]. These studies also show the importance of the pyrolysis heating programme. Mass is lost from the film above 150 °C, and between 250 and 500 °C, there is the greatest loss of mass from the photoresist film as oxygen and nitrogen species are removed and carbonisation begins. At temperatures above 600 °C graphitisation occurs and the films begin to display nanocrystalline structures that have a significant contribution from both sp^2 and sp^3 type carbon [11, 20]. Consistent with these structural changes in PPF, the rate of electron transfer increases as pyrolysis temperatures are increased [17].

Pyrolysis of photoresist in inert environments, either under vacuum, N_2, H_2 or forming gas, lead to low oxide surfaces. In the case of pyrolysis under vacuum, the surfaces produced have the lowest O/C ratio of all. However, these films cannot be heated to temperatures above 1,000 °C [21] and the final PPF films have higher resistance than those pyrolysed at 1,100 °C. A way to combat this is to use forming gas as the PPF produced has similarly low O/C ratio, but this process allows the films to be heated to higher temperatures with the concomitant lower film resistance [12]. A 10% increase in mass loss is seen between PPF samples pyrolysed in H_2 rather than N_2 [13, 20]. Different gas flows have also been used for the fabrication of PPF films: 0.1 L min^{-1} by McCreery and 6 L min^{-1} by Downard and co-workers [8, 10].

There are two heating programmes commonly used for pyrolysing photoresist. The first is the continuous heating of the photoresist directly to the required temperature at a constant rate (e.g. 10 or 5 °C/min) as performed by McCreery [10] and Kinoshita [22]. The second method is in a three-step heating programme used by Downard and co-workers [23]. In this temperature programme, the temperature is increased to a certain point and held there for a set amount of time. This process is repeated twice more until the temperature reaches 1,050 °C [23].

Increasing electrochemical uses of PPF films leads to a need to understand and control properties imparted during fabrication [18, 19]. Our main interest is in developing electrochemical sensors using organic modification layers. In such cases, the underlying electrode is required to offer good electron transfer kinetics and a smooth surface. The attractiveness of PPF is the smoothness of the surface and that it is compatible with modification using aryl diazonium salts derived layers [8, 24–26]. This paper explores the effects of

Table 1 Levels of seven factors in eight preparations of a PPF electrode in a randomised Plackett–Burman experimental design

Run	T_1/°C	T_2/°C	T_3/°C	t_1/min	t_2/min	t_2/min	Position
1	500(+)	680(+)	1,050(−)	40(−)	15(+)	90(+)	Centre (−)
2	550(−)	750(−)	1,050(−)	40(−)	30(−)	60(−)	Centre (−)
3	550(−)	750(−)	1,050(−)	20(+)	15(+)	90(+)	End (+)
4	500(+)	750(−)	1,100(+)	20(+)	30(−)	90(+)	Centre (−)
5	500(+)	680(+)	1,050(−)	20(+)	30(−)	60(−)	End (+)
6	550(−)	680(+)	1,100(+)	20(+)	15(+)	60(−)	Centre (−)
7	550(−)	680(+)	1,100(+)	40(−)	30(−)	90(+)	End (+)
8	500(+)	750(−)	1,100(+)	40(−)	15(+)	60(−)	End (+)

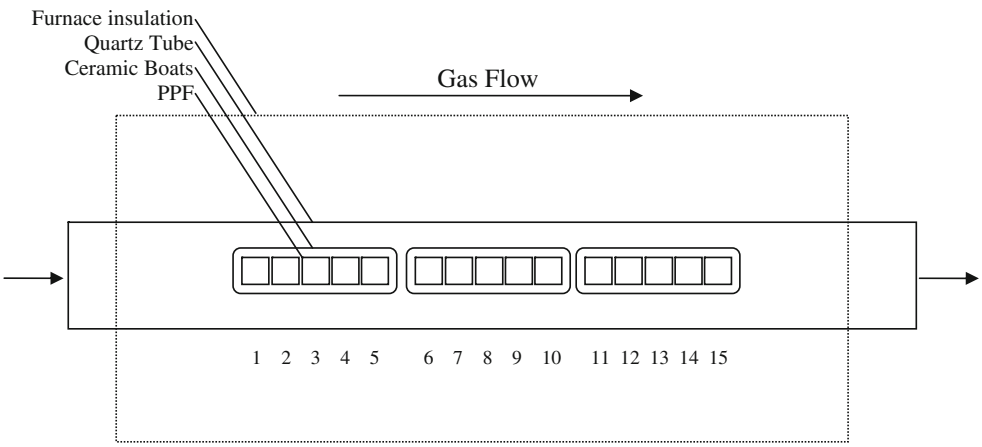

Fig. 1 Position of samples in the furnace

different variables used during the three-step pyrolysis programme. Physical parameters of the films such as resistivity, film thickness and roughness were measured, as well as electrochemical properties using a range of redox species to provide information on surface oxides, surface contamination and heterogeneous electron transfer kinetics.

For complex systems such as the one investigated here, there are too many factors to investigate by traditional 'change one factor at a time' methods. Here, we demonstrate the use of a simple screening design which allows us to study seven factors in only eight experiments. Even with these few experiments the effect of each factor is obtained as the average of four comparisons. Plackett–Burman designs [27] are highly fractionated two-level designs that give main (independent) effects only. They require $4n$ experiments to obtain $4n-1$ main effects. Although the design gives no information about interactions among effects (which could well exist in the present system), and cannot offer optima of responses, they are valuable as a first step to understanding how changes in influence factors affect the characteristics of the carbon films. The efficiency of the design is particularly important when there is a cost, in time or money, in performing an experiment at a set of conditions. Here, the fabrication of a PPF electrode takes several hours, to which must be added the subsequent characterisation.

Two values (coded '−' and '+' in the design shown in Table 1) are chosen for each factor. When a response (e.g. resistivity) is measured for each experiment, the main effect of a factor is calculated by summing over all experiments the product of the coded level of the factor (+1 or −1) and the response, and then dividing this sum by 4 (half the number of experiments). The main effect has the units of the response variable and is the average change in the variable when that factor goes from its '−' value to its '+' value. By convention, the '−' level of a factor is the usual value applied in experiments and the '+' is a value that is chosen to be sufficiently different to cause a measureable change in the response (if indeed the factor causes a change), but not so great as to take the experiment into nonsensical factor values. To confound the effects of uncontrolled variables, the order of performing the experiments is randomised.

Materials and methods

Chemicals

All chemicals were used as received. Potassium ferricyanide and ruthenium hexaamine were purchased from Aldrich (Sydney, Australia). Potassium chloride was obtained from Fluka (Sydney, Australia). $(NH_4)_2SO_4FeSO_4{\cdot}6H_2O$ and 70% $HClO_4$ was purchased from Ajax Chemicals (Sydney, Australia). Three-inch <100> n-type silicon wafer (500–550 μm thick and 2.0–9.0 Ω cm resistivity) was purchased from Micro Materials and Research Consumables (Mt. Waverly, Melbourne). Positive photoresist AZ 4620 was purchased from AZ Electronic Materials (Tokyo, Japan). Forming gas was purchased from Air Liquide (Sydney, Australia).

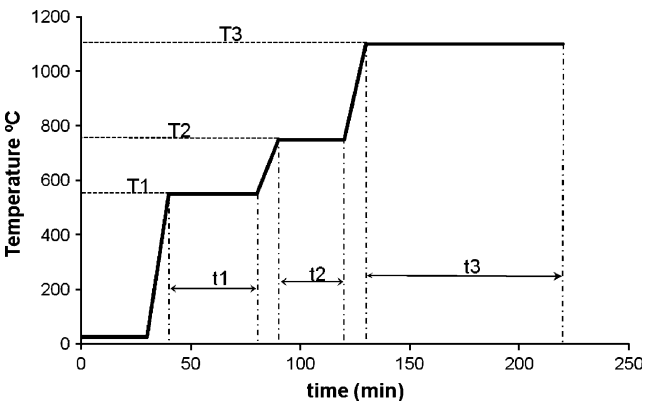

Fig. 2 Heating profile for pyrolysis of photoresist films. *T1*, *T2* and *T3* refers to heating temperatures and *t1*, *t2* and *t3* refers to heating times

Table 2 Measured values of response variables for preparation of PPF electrodes with a gas flow rate of 600 mL/min (all cyclic voltammetry was scanned at 100 mV s^{-1})

Run	$\Delta E_p Fe(CN)_6^{3-/4-}$ /mV	$\Delta E_p Ru(NH_3)_6^{2+/3+}$ /mV	ΔE_p $Fe^{2+/3+}$/mV	Resistivity/(mΩ cm)	Roughness/nm
1	105	88	579	3.82	0.38
2	413	276	564	4.22	0.44
3	400	107	337	11.00	0.44
4	322	195	432	5.85	1.15
5	215	327	542	9.68	1.29
6	134	110	457	3.72	0.98
7	969	127	610	6.51	3.33
8	383	103	149	5.46	8.54

PPF preparation

A 3-in <100> n-type silicon wafer was cut into 1.4×1.4 cm^2 pieces using a diamond scribe. The wafer pieces were then cleaned by sonicating in successive baths of acetone, methanol and isopropanol. These samples were then dried with nitrogen. Under yellow light, positive photoresist AZ 4620 was spin coated (3–4 drops/0.3–0.5 mL) onto the wafer pieces at 3,000 rpm for 30 s. The wafer pieces were then heated at 95 °C for 20 min to remove excess solvent but the films were still soft to touch. The samples were then kept overnight at 45 °C.

The photoresist-coated wafer pieces were placed in three ceramic boats, five wafer pieces per boat. The boats were then placed in the furnace as shown in Fig. 1. The furnace was flushed with forming gas for 30 min before the pyrolysis programme was started. Pyrolysis proceeded with forming gas flowing through the tube continuously at a flow speed of either 600 or 0.64 mL min^{-1}. The pyrolysis programmes used are shown in Table 1. The PPF samples were then left to cool down to room temperature slowly whilst still under forming gas. The PPF samples were removed and placed under vacuum until used.

Physical characterisation of films

Resistance of the PPF was measured using copper conducting wires set in a square arrangement 1 by 1 cm with reproducible pressure of the copper wires onto the carbon surface [28]. The sheet resistance (R) for each PPF film was calculated as the average of four independent measurements. Resistivity (ρ) is

$$\rho = \frac{(R - R_{Cu}) \times w \times d}{L} \quad (1)$$

where R_{Cu} is the internal resistance of the copper bars, w is the distance between copper bars, L is the length of each bar (measured with vernier callipers) and d is the film thickness. Film thickness was obtained using a Sloan Dektak II profilometer. Three PPF samples, one from each end of the furnace and one from the middle, were scratched down to the substrate using a needle, and the depth of the scratch was measured three times in different places and the average of these was calculated.

AFM was performed on a Digital Instruments Dimension 3000 AFM in tapping mode. Images of 10 by 10 μm were recorded and used for all roughness data presented herein.

Electrochemical characterisation

Electrochemical measurements were carried out using an Autolab potentiostat with a Ag/AgCl/3.0 M KCl reference electrode and a platinum wire counter electrode in a custom-made electrochemical cell which gives a controlled area of PPF by allowing only a disc with a 3 mm diameter to be exposed. The redox systems used were 1.0 mM $Ru(NH_3)_6^{2+/3+}$

Table 3 Measured values of response variables for preparation of PPF electrodes with a gas flow rate of 0.64 mL/min (all cyclic voltammetry was scanned at 100 mV s^{-1})

Run	$\Delta E_p Fe(CN)_6^{3-/4-}$ /mV	$\Delta E_p Ru(NH_3)_6^{2+/3+}$ /mV	ΔE_p $Fe^{2+/3+}$/mV	Resistivity/(mΩ cm)	Roughness/nm
1	918	134	806	2.40	2.75
2	820	115	571	3.13	5.17
3	132	122	357	6.60	0.67
4	632	68	615	1.93	1.92
5	649	115	610	15.10	0.76
6	264	186	782	1.93	1.34
7	737	176	664	5.05	23.59
8	474	110	550	0.43	0.90

Table 4 Main effects for preparation of PPF electrodes with a gas flow rate of 600 mL/min (all cyclic voltammetry was scanned at 100 mV s^{-1})

Response variable	T_1	T_2	T_3	t_1	t_2	t_2	Position
$\Delta E_p Fe(CN)_6^{3-/4-}$/mV	223	24	169	200	224	163	248
$\Delta E_p Ru(NH_3)_6^{2+/3+}$/mV	−23	7	−66	−37	129	−74	−1
ΔE_p $Fe^{2+/3+}$/mV	266	−706	−374	134	628	247	−393
Resistivity/(mΩ cm)	0.16	0.70	−1.79	−2.56	0.57	1.02	3.76
Roughness/nm	1.56	−2.22	0.83	−3.14	−1.21	−2.58	−1.62

in 1.0 M KCl from $Ru(NH_3)_6Cl_3$; 1.0 mM $Fe(CN)_6^{3-/4-}$ in 1.0 M KCl from $K_3Fe(CN)_6$ and 1.0 mM $Fe^{2+/3+}$ in 0.2 M $HClO_4$ from $(NH_4)_2SO_4FeSO_4{\cdot}6H_2O$ and 70% $HClO_4$. All solutions were made in Milli-Q water (resistivity >18 MΩ cm). All solutions were degassed with dry nitrogen for 10 min prior to use. For each redox probe, five cycles at 100 mV s^{-1} were run employing cyclic voltammetry.

Glassy carbon

GC electrodes were obtained from Bioanalytical Systems (West Lafayette, IN, USA) and were 3 mm diameter rods encased into solvent-resistant epoxy resin. The electrodes were hand-polished successively in 1.0, 0.3, and 0.05 μm alumina slurries (5 min each) made from dry Buelher alumina (Buelher, Lake Bluff, IL, USA) and Milli-Q water on microcloth pads (Buelher). The electrodes were thoroughly rinsed with Milli-Q water and sonicated for 5 min after the final polish.

Experimental design

A Plackett–Burman seven-factor screening design (Table 1) was used to investigate six heating parameters and the position of the sample in the heating tube (centre, ends). Two flow rates were also investigated (0.64 and 600 mL min^{-1}) in separate Plackett–Burman designs. Five response variables were measured: three cyclic voltammetry peak separations [$\Delta E_p Ru(NH_3)_6^{2+/3+}$, $\Delta E_p Fe(CN)_6^{3-/4-}$, ΔE_p $Fe^{2+/3+}$] and the resistivity and the roughness of the carbon film. Measurement of peak separation provides information on heterogeneous electron transfer kinetics and, indirectly, on surface oxides (ΔE_p $Fe^{2+/3+}$) and surface cleanliness [$\Delta E pFe(CN)_6^{3-/4-}$].

Choice of factor values

The staggered heating programme of Downard and co-workers [8, 23] is used which gives six factors to be investigated, three times and three temperatures as shown in Fig. 2. The three temperatures were chosen as they fall into roughly the three areas of the pyrolysis process. Between 250 and 500 °C, the greatest mass loss occurs during pyrolysis [21]. Carbonisation starts from 600 °C [11], and it has been shown that the best result in terms of resistance and electron transfer for final pyrolysis temperatures is between 1,000 and 1,100 °C. Table 1 gives the values corresponding to the Plackett–Burman levels −1 and +1.

In addition, the last factor in the design was the position of the PPF in the furnace. The positions of the PPF and direction of gas flow are schematically illustrated in Fig. 1. Two gas flows were chosen in this study, 0.64 and 600 mL min^{-1}, with the full Plackett–Burman design being repeated at each gas flow.

Results and discussion

The number of potential factors in the production of a PPF film that can be studied (several temperatures, times, flow rate and position) requires a carefully designed experimental campaign. The chosen Plackett–Burman design minimises the number of experiments at the expense of knowledge of two-way and higher order interactions [29]. As with all experimental designs, the random variation in the response variables arising from uncontrolled factors in the experiment must be minimised, as any effect that is less than the random variation might not be identified as significant. The raw results from the response variables measured (voltam-

Table 5 Main effects for preparation of PPF electrodes with a gas flow rate of 0.64 mL/min (all cyclic voltammetry was scanned at 100 mV s^{-1})

Response variable	T_1	T_2	T_3	t_1	t_2	t_2	Position
$\Delta E_p Fe(CN)_6^{3-/4-}$/mV	−180	−128	−103	318	263	53	−160
$\Delta E_p Ru(NH_3)_6^{2+/3+}$/mV	43	−49	13	11	−19	−6	5
ΔE_p $Fe^{2+/3+}$/mV	−52	−192	67	57	−9	−18	−148
Resistivity/(mΩ cm)	−0.79	−3.10	−4.47	−3.64	3.46	−1.15	4.45
Roughness/nm	6.11	−4.94	4.60	6.93	6.45	5.19	3.68

metric peak separation for $Fe(CN)_6^{3-/4-}$, $Ru(NH_3)_6^{2+/3+}$ and $Fe^{2+/3+}$, the films resistivity and film roughness) for the two flow rates are shown in Tables 2 and 3.

The main effects are calculated from this data and shown in Table 4 for the faster flow rate and Table 5 for the slower flow rate. The signs have been adjusted to show the effect of moving from the smaller value to the greater value. In the case of position, the 'positive' direction of the change is from middle to edge.

Some of the more evident effects are discussed here. Position in the furnace has the greatest effect on ΔE_p $Fe(CN)_6^{3-/4-}$, making the peak separation greater, but reducing the peak separation for ΔE_p $Fe^{2+/3+}$ at the faster flow rate. For ΔE_p $Fe^{2+/3+}$, the peak separation decreases, and hence, the rate of electron transfer increases, at the higher gas flow. For most variables, the effect of the change of factor level is reduced when there is a slower flow. We also found that the reproducibility of the responses was better for the slower flow rate. The peak separation of the ruthenium couple was the most unstable.

Uncertainty in preparation and measurement

Where possible, the repeatability of the measurement of each response has been estimated from replicate measurements on a single prepared electrode. Their values are reflected in the significant figures reported for the results in Tables 2 and 3. For example, for the first run with a slow gas flow, the repeatability relative standard deviation of the resistivity for all positions in the furnace was 2.7% (n=4). Typical confidence intervals calculated from these data are shown in Fig. 3. There is an art in preparing reproducible electrodes that depends critically on day-to-day variations in gas flow, temperature, position in the furnace and so on. The data given here reflects this, but despite the variability, it does allow some conclusions to be drawn.

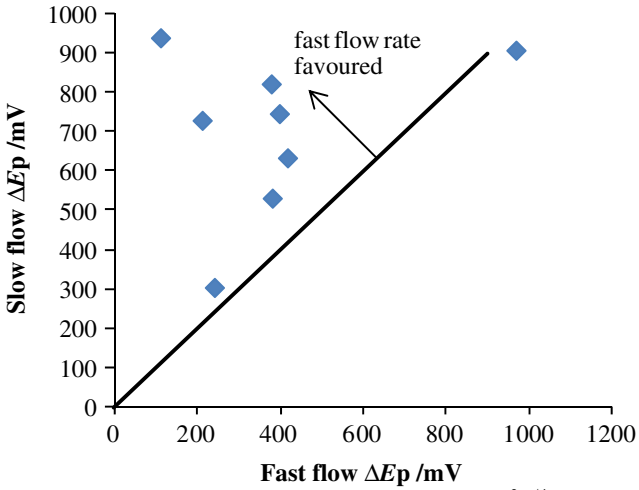

Fig. 4 Peak separation for the redox couple $Fe(CN)_6^{3-/4-}$ for the eight Plackett–Burman design points, for fast and slow gas flows. *Points* above the line of equality show that a smaller peak separation is favoured by the fast flow rate

Physical characteristics of PPF samples

In general, it can be seen that the resistivity of the films is greatly affected by the position of the sample within the furnace (Fig. 3). The heating capacity of the furnace is at a maximum in the middle of the tube; although, according to the supplier of the furnace, the heat should be uniform within the region in which the PPF samples are located (i.e. the heat in the centre of the tube should be the same within 4 cm of either end of the tube). It can be seen that positioning at the ends of the furnace leads to greater resistivity, while a higher temperature during the carbonisation step (T_2) gave smaller roughness values. It is, however, important to note that, within this range of resistivity, there is no direct correlation with the electron transfer rate as can be seen in Table 2. Furthermore, it is clear from Table 2 that the rate of gas flow

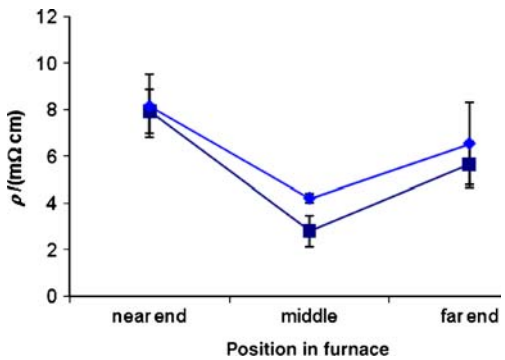

Fig. 3 Resistivity of electrodes prepared from PPF carbon films as a function of position in the furnace. *Error bars* are 95% confidence intervals of the mean of four separate measurements. *Upper line*, flow rate 600=mL min^{-1}; *lower line*, flow rate=0.64 mL min^{-1}

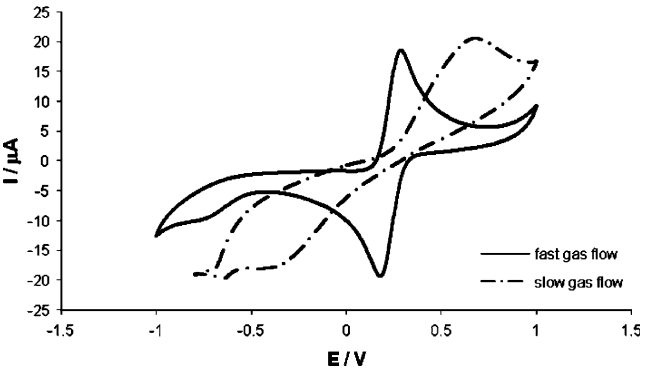

Fig. 5 Cyclic voltammograms of run 1 preparations conditions under different gas rates in 1 mM $Fe(CN)_6^{3-/4-}$, 1 M KCl scanned at 100 mV s^{-1} vs Ag/Ag^+ (*solid line*, 600=mL min^{-1}; *dashed line*, flow rate=0.64 mL min^{-1})

Table 6 Comparisons of electron transfer rate constant for certain redox probes calculated from ΔEp according to the Nicholson method [35])

	This study			PPF [10]	PPF [8]
	PPF Gas flow 0.64 mL min^{-1}	PPF Gas flow 600 mL min^{-1}	GC		
$k_s Fe(CN)_6^{3-/4-} / 10^{-6} cms^{-1}$	1,300	7,000	400	100	1,500
$k_s Ru(NH_3)_6^{2+/3+} / 10^{-6} cms^{-1}$	300	3,200	200	200	2,600
k_s $Fe^{2+/3+}/10^{-6}$ cm s^{-1}	15,700	18,200	34,100	210,000	–

does not influence the resistivity. Resistivity in slower gas flows was favoured by higher temperature and longer times for t_1 and t_3. At higher flow rate, the position was less clear.

Film thickness is also not affected by either gas flow or heating parameters. Within the variables assessed, film thickness is only influenced by the initial amount of photoresist spin coated onto the silicon wafer and the spin speed. Conversely, roughness is affected by the gas flow. Roughness generally increased (the main effect was positive) at the slower flow rate, as can be seen by comparing Tables 2 and 3, while at the greater flow rate, longer pyrolysis times promoted negative main effects. For each flow rate, higher T_1 and T_3 favoured greater roughness.

Electrochemical characteristics of PPF samples

It can be seen that the effects on $\Delta E_p Ru(NH_3)_6^{2+/3+}$ are smaller than the other couples. As ΔE_p is indicative of the kinetics of electron transfer [30], this result is consistent with our knowledge of the electrochemistry as the $Ru(NH_3)_6^{2+/3+}$ couple is regarded as truly outer sphere, and hence, the electrochemistry should not be greatly influenced by the nature of the surface of the electrode [31, 32]. The $Fe(CN)_6^{3-/4-}$ couple is classed as inner sphere but insensitive to surface oxides. $Fe(CN)_6^{3-/4-}$ is, however, sensitive to surface cleanliness in regards to adventitious impurities [31–34]. These results provide an indication that the range of resistivities

Table 7 General guidelines for PPF surface properties

Desired surface properties	Temp 1 (°C) T_1	Temp 2 (°C) T_2	Temp 3 (°C) T_3	Time 1 (min) t_1	Time 2 (min) t_2	Time 3 (min) t_3	Gas flow mL min^{-1}	General statements
Fast electron transfer Clean surface, Low surface roughness <0.6 nm	550	680	1,100	20	15	60	600 (fast)	High final temperature for a shorter time
Fast electron transfer Clean surface, Higher surface roughness >1.0 nm	500	680	1,050	40	15	90	600 (fast)	Lower final temperature for a longer time
Low surface oxide Low surface roughness <0.6 nm	500	680	1,050	20	30	60	600 (fast)	Low T2, and T1 held for a short time
Low surface oxide Higher surface roughness >1.0 nm	550	680	1,100	40	30	90	600 (fast)	Low T2, and T1 held for a longer time
Higher surface oxide Low surface roughness <0.6 nm	550	750	1,050	20	15	90	600 (fast)	High T2
Fast electron transfer Rough surface	550	750	1,050	40	30	60	0.64 (slow)	Generally the same trends occur for the slower gas flow but the surfaces are rougher

observed as a function of position in the tube furnace does not have a significant effect on the electron transfer kinetics. In comparison, ΔE_p for the $Fe(CN)_6^{3-/4-}$ couple is, for the majority of runs, lower at the faster gas flow rate (Fig. 4), as seen by comparing values of ΔE_p for the same run number at the two different gas flow rates. An example of the electrochemical behaviour is illustrated in Fig. 5 for the two different gas flow rates for run 1. In general, the 'pattern' of ΔE_p of $Fe(CN)_6^{3-/4-}$ was repeated throughout both gas flow rates, which indicates that the heating parameters have some influence on the response of $Fe(CN)_6^{3-/4-}$.

A comparison with other studies is made for the surface with the fastest rate of electron transfer for $Fe(CN)_6^{3-/4}$, run 1 for the 600-mL min^{-1} flow rate, is presented in Table 6. The electron transfer rates are comparable to those obtained for previous studies carried out by the groups of both McCreery [10] and Downard [8] for their best set of conditions for PPF fabrication. McCreery and co-workers have also noted that the ΔE_p of $Ru(NH_3)_6^{2+/3+}$ were slightly greater on PPF (k° 0.020 cm s^{-1}) than on GC (k° 0.037 cm s^{-1}) [10], which is contrary to our observations.

To examine the oxide content, the redox probe $Fe^{2+/3+}$ was used, as it has been shown that as oxide content increases on the surface, the rate of electron transfer increases [32, 34]. It was seen that, in general, the runs with the higher T_2 of 750 °C had a greater ΔE_p for $Fe^{2+/3+}$. It was observed that the ΔE_p for $Fe^{2+/3+}$ did not correlate with either fast or slow electron transfer kinetics for $Fe(CN)_6^{3-/4-}$, thus implying that there is no correlation between surface cleanliness and oxide content.

The trend in ΔE_p for $Fe^{2+/3+}$ was also seen in the pyrolysis runs with a slower gas flow rate; those runs with a lower T_2 showed higher ΔE_p values. It was also observed that the change in gas flow does not significantly influence the surface oxides (see Tables 2 and 3).

Experimental design

The information obtained by the experiments described here could have been provided in a more efficient manner by a 12-experiment, 11-factor Plackett–Burman design (i.e. the next in the 4*n* series, n=3). In these eight factors, namely, three times, three temperatures, position and flow rate could have been investigated, with the remaining three factors being 'dummy' variables to give estimates of the variance of factor effects directly. However, at the planning stage, there was sufficient interest in the effect of flow rate that it was decided to obtain more information on this factor, as described.

A main effect design, as used here, cannot give information about correlations among factors. It is expected that time and temperature will be correlated; to some extent, higher temperatures can be traded off against longer times. Factorial or composite designs can give such information at the expense of a greater number of experiments.

Conclusion

The use of the Plackett and Burman design makes it possible to study the influence of the different factors on the final PPF produced and has served as a guide to the types of experiments to perform. However, from the results presented in Tables 2 and 3, it is clear there is a high degree of variability between runs, which compromises the depth of information that can be extracted from the design. However, general trends can be observed and the important and unimportant factors identified. This information allows fabrication guidelines for PPF to be stated for specific end-user requirements (Table 7). If the surface roughness and cleanliness are not important but good electron transfer kinetics are, then fast gas flow rates are not needed. Faster gas flow rates will, however, give far cleaner surfaces with continued good transfer kinetics. Further surface characteristics such as surface roughness and oxide content can be controlled through heating variables, as seen in Table 7.

References

1. McCreery RL, Cline KK (1996) In: Kissinger PT, Heineman WR (eds) Laboratory techniques in electroanalytical chemistry. Marcel Dekker, New York, p 293
2. Downard AJ (2000) Electroanalysis 12:1085
3. Gooding JJ, Mearns F, Yang W, Lui J (2003) Electroanalysis 15:81
4. Jenkins GM, Kawamura K (1971) Nature 231:175
5. Hui CZ, Feng L, Andrade JD (1988) Carbon 26:543
6. Rothwell WS (1968) J Appl Phys 39:1840
7. Saxena RR, Bragg RH (1978) J Non-Cryst Solids 28:45
8. Brooksby PA, Downard AJ (2004) Langmuir 20:5038
9. Anariba F, DuVall SH, McCreery RL (2003) Anal Chem 75:3837
10. Ranganathan S, McCreery RL (2001) Anal Chem 73:893
11. Kostecki R, Schnyder B, Alliata D, Song X, Kinoshita K, Kotz R (2001) Thin Solid Films 396:36
12. Ranganathan S, McCreery RL, Majji SM, Madou M (2000) J Electrochem Soc 147:277
13. Lyons AM, Wilkins CW Jr , Robbins, M (1983) Thin Solid Films 103:333
14. Yu SSC, Downard AJ (2005) J Surf Sci Nanotechnol 3:294
15. Lyons AM (1985) J Non-Cryst Solids 70:99
16. Lum R, Wilkins CW Jr, Robbins M, Lyons AM, Jones RP (1983) Carbon 21:111
17. Kim J, Song X, Kinoshita K, Madou M, White R (1998) J Electrochem Soc 145:2314
18. Park BY, Taherabadi L, Wang C, Zoval J, Madou MJ (2005) J Electrochem Soc 152:J136
19. Singh A, Jayaram J, Madou MJ, Akbar S (2002) J Electrochem Soc 149:E78
20. Lyons AM (1985) J Non-Cryst Solids 70:99
21. Ranganathan S, McCreery RL, Majji SM, Madou M (2000) J Electrochem Soc 147:277
22. Kostecki R, Song X, Kinoshita K (1999) Electrochem Solid-State Lett 2:465
23. Brooksby PA, Downard AJ (2005) Langmuir 21:1672
24. Yu SSC, Downard AJ (2005) e-J Surf Sci Nanotechnol 3:294
25. Yu SSC, Downard AJ (2007) Langmuir 23:4662

26. McCreery RL, Dieringer J, Osman Solak A, Snyder B, Nowak AM, McGovern WR, DuVall S (2003) J Am Chem Soc 125: 10748
27. Plackett RL, Burman JP (1946) Biometrika 33:305
28. Brooksby PA, Downard AJ, Yu SSC (2005) Langmuir 21:11304
29. Hibbert DB (2007) Quality assurance for the analytical chemistry laboratory. Oxford University Press, Oxford
30. Nicholson RS (1965) Anal Chem 37:1351
31. Kneten Cline KR, McDermott MT, McCreery RL (1994) J Phys Chem 98:5314
32. McCreery RL, Cline KK, McDermott CA, McDermott MT (1994) Colloids Surf A 93:211
33. McCreery RL (1999) In: Wieckowski A (eds) Interfacial electrochemistry. Marcel Dekker, New York
34. Chen P, McCreery RL (1996) Anal Chem 68:3958
35. Nicholson RS (1965) Anal Chem 37:1351